

Vertical Migration of the Toxic Dinoflagellate *Karenia Brevis* and the Impact on Ocean Optical Properties

Oscar Schofield and John Kerfoot
Coastal Ocean Observation Laboratory, Institute of Marine and Coastal Sciences, Rutgers
University,
New Brunswick, New Jersey, USA

Kevin Mahoney
Department of Marine Science, University of Mississippi,
Stennis Space Center, Mississippi, USA

Mark Moline
Department of Biology, California Polytechnic State University,
San Luis Obispo, California, USA

Matthew Oliver
Coastal Ocean Observation Laboratory, Institute of Marine and Coastal Sciences, Rutgers
University,
New Brunswick, New Jersey, USA

Steven Lohrenz
Department of Marine Science, University of Mississippi,
Stennis Space Center, Mississippi, USA

Gary Kirkpatrick
Mote Marine Laboratory,
Sarasota, Florida, USA

Abstract

Vertical migration behavior is found in many harmful algal blooms; however, the corresponding impact on ocean optical properties has not been quantified. A near-monospecific population of the dinoflagellate *Karenia brevis* was encountered off the west coast of Florida. The community was tracked for 24 hours by following a Lagrangian drifter deployed at the beginning of the experiment. A suite of inherent optical and cellular measurements was made. Over the 24 hour period, the *K. brevis* population increased during the day with concentrations peaking in the late afternoon (1600 local daylight time) in the upper 2 m of the water column.

The increase in *K. brevis* in surface waters resulted in enhanced reflectance at the sea surface with distinct spectral changes. There was a 22% decrease in the relative amount of the green reflectance due to increased pigment absorption. There was enhanced red (35%) and infrared (75%) light reflectance due to the increased particle backscatter and chlorophyll a fluorescence; however, the relative impact of the fluorescence was relatively small despite high cell numbers due to the significant fluorescence quenching present in *K. brevis*. The relative change in the blue light reflectance was not as large as the change in green light reflectance, which is surprising given the pigment absorption in the blue wavelengths of light. The increased blue light pigment absorption was offset by a significant decrease in nonalgal particle absorption. The inverse relationship between *K. brevis* and nonalgal particles was robust. This relationship may reflect low grazing on *K. brevis* populations due to the neurotoxins associated with this dinoflagellate. The low-grazing pressure may provide the mechanism by which this slow-growing dinoflagellate can achieve high cell numbers in the ocean.

Keywords: optics, Red Tide.

Introduction

Blooms of the toxic red tide dinoflagellate *Karenia brevis* (formerly *Gymnodinium breve* and *Ptychodiscus brevis*) occur annually in the Gulf of Mexico [Steidinger et al., 1998]. The intensity and spatial extent of the blooms vary year by year. These blooms are an important water quality parameter for the west coast of Florida as *K. brevis* cells produce brevetoxins [Steidinger et al., 1973; Carder and Steward, 1985; Riley et al., 1989; Pierce et al., 1990;

Shumway et al., 1990]. These brevetoxins cause death in bird, fish, and marine mammals [Landsberg and Steidinger, 1998]. Additionally, brevetoxins once volatilized into marine aerosols irritate human respiratory systems [Hemmert, 1975; Asai et al., 1982; Kirkpatrick et al., 2004]. Management strategies for monitoring red tides primarily rely on the collection of discrete samples, thus have limited temporal and spatial resolution. Therefore much effort has focused on developing the ability to map harmful algal blooms using noninvasive optical and remote-sensing approaches [Schofield et al., 1999].

Modeling studies focused on inverting remote-sensing reflectance into the respective phytoplankton taxa shows promise [Carder and Steward, 1985; Mahoney, 2003; Roesler et al., 2006]. This is especially true for *K. brevis* because of its unique absorption properties [Millie et al., 1995, 1997; Lohrenz et al., 1999; Kirkpatrick et al., 2000] and low backscattering coefficients [Mahoney, 2003; Kerfoot et al., 2005; Cannizzaro, 2004]. The degree with which the *K. brevis* signal can be isolated will also be dependent on the presence of other optically active constituents such as colored dissolved organic matter (CDOM), nonalgal particles (usually dominated by detritus), and the position of *K. brevis* within the water column.

Many toxic dinoflagellates exhibit significant vertical migration which impacts both the autotrophic communities and the corresponding ecosystem. The environmental factors that influence the vertical migration in dinoflagellates are light [Eppley et al., 1968; Forward, 1970], temperature [Kamykowski, 1981], salinity [Kamykowski, 1981], and nutrients [Holmes et al., 1967; Eppley et al., 1968; Kamykowski, 1981; Tyler and Seliger, 1981]. The physiological factors regulating the behavior are circadian rhythms [Forward and Davenport, 1970], cell cycle phenomena [Kamykowski, 1995], biochemical pools and synthesis rates [Cullen, 1985;

Kamykowski and Yamazaki, 1997]. *K. brevis* exhibits a positive phototactic vertical migration [Heil, 1986; Steidinger, 1975], and cells often concentrate (as great as 1×10^8 cells L^{-1}) at the air-sea interface. While studies on the underlying biology are advancing, studies documenting the impact of vertical migration of *K. brevis* on environmental optics are few. This is unfortunate as the net result of the vertical migration is that it will discolor the water and thus significantly impact remote-sensing approaches.

During a cruise in the Gulf of Mexico a population of *K. brevis* was encountered. Over a 24 hour period, we tracked the impact of the *K. brevis* vertical migration on the water column optical properties and remote-sensing reflectance. Our results illustrate the degree that the vertical migration and the optical constituents associated with *K. brevis* impact remote-sensing reflectance. The associated changes in the optical properties reflected the concentrated *K. brevis* population right at the ocean-atmosphere interface and the low concentration of nonalgal particles associated with the red tide population.

Methods

2.1. Field Data

--- INSERT FIGURE 1 ---

A research cruise aboard the R/V Suncoaster was conducted off the west coast of Florida from 19 to 26 October (Figure 1). The cruise consisted initially of a mesoscale survey conducted to locate a population of *K. brevis*. The survey portion of the cruise consisted of discrete stations which were analyzed for the presence of *K. brevis* by microscopic cells counts on water samples.

Stations were chosen from real-time data provided by flow-through instruments attached to the ship's surface seawater intake system. The flow-through sensors included a Turner chlorophyll fluorometer and a colored dissolved organic matter (CDOM) absorption mapping system. The CDOM mapping system [Kirkpatrick et al., 2003] consisted of a liquid waveguide capillary cell (LWCC, World Precision Instruments, Inc.) coupled to a fiber-optic spectrometer (S2000, Ocean Optics, Inc.) and a fiber-optic xenon flashlamp (PS-2, Ocean Optics, Inc.). Water was pumped by miniature peristaltic pump (P625, Instech Laboratories, Inc.) through size fractionation and cross-flow filters (MicroKros, Spectrum Laboratories, Inc.) and then through the LWCC for optical density spectra measurements. Details regarding the LWCC operation procedures can be found in work by Kirkpatrick et al. [2003]. The system was set up only to collect data from the ship's water intake and therefore only data near the surface was collected. Changes in the data collected by the flow-through system resulted in the ship occupying a station and discrete samples were collected throughout the water column. Microscope analysis was then used to assess if *K. brevis* was present in the water column, and if no cells were observed then the ship continued its survey.

On 22 October a patch of *K. brevis* was located and a radio-telemetered Lagrangian drifter was deployed allowing bloom patch to be followed over the diel cycle. The near-surface drifter (Brightwaters Instruments Corp., model 104V) is similar to the Coastal Ocean Dynamics Experiment (CODE) drifter that has been used to track bloom patches. The drifter sails were set to span the depth range from 0.3 m to 1 m to couple the drifter to the near-surface layer of the water column and its entrained bloom population. The drifter broadcast its GPS position at regular intervals to the ship via VHF radio making it possible to relocate it without having to maintain constant visual contact. With this approach it was possible to track and sample the

bloom patch for 24 hours as it was advected by surface currents. The patch remained in shallow water (<15 m) throughout the diel experiment.

During the diel cycle, physical and optical measurements were made hourly with a profiling instrument cage. Optical profiles consisted of a WET Labs Inc. absorption/attenuation meter (ac-9) and a Falmouth CTD. The ac-9 instrument was outfitted with the standard nine wavelengths (412, 440, 488, 510, 555, 630, 650, 676, 715 nm). The ac-9 optical windows and flow cells were cleaned prior to each deployment. At each station, the instrument was lowered to depth and the instrument was allowed to equilibrate to ambient temperature before data were collected. Only data from the upcasts were utilized in order to ensure that air bubbles were flushed from the tubes. There were no significant differences in the upcasts or downcasts for depths greater than 1 m. The upcast data was cleaner than the downcast data in the upper meter of the water column. The water was drawn through the ac-9 with a SBE pump. Data were averaged into 0.25-m depth bins for all subsequent analyses. The instruments were factory calibrated prior to the field season. Manufacturer recommended protocols were used to track instrument calibration. Salinity and temperature corrections based on CTD were applied [Pegau et al., 1997]. Whenever possible daily clean water calibrations were conducted; however, sampling schedules did not always allow for a daily calibration. Under these circumstances the most recent water calibration was used. It should be noted that the maximum period without a calibration was two days. The drift during this study was negligible (<3%) and the accuracy of the ac-9 data was $\pm 0.01 \text{ m}^{-1}$.

A Satlantic Inc. HyperTethered Spectral Radiometric Buoy was deployed during the daylight hours to provide hyperspectral (~3 nm resolution) measurements of sea surface

reflectance [$R(\lambda)$] that was estimated from the above water downwelling irradiance [$E_d0^+(\lambda)$] and the upwelling radiance measured 0.75 m below the sea surface [$L_u(\lambda)$]. For these deployments the buoy was floated away from the ship, to avoid ship shadow, and the irradiance was recorded for at least 15 min. Radiometric data was processed using Satlantic's Prosoft software package using the manufacturer protocols. The manufacturer software propagates $L_u(\lambda)$ through the ocean surface allowing the reflectance to be calculated as $R(\lambda) = L_u0^+(\lambda)/E_d0^+(\lambda)$. This propagation requires estimates of the diffuse attenuation coefficient (K) to estimate the light attenuated in the upper 0.75 m of the water column. Prosoft uses the Austin and Petzold [1981] model to derive K at 443 and 550 nm which is used to estimate in situ pigment concentrations which can then be inverted to provide a spectral estimate of K using the empirical model derived by Morel [1988].

At each station during the diel study, water was collected with Niskin bottles primarily from the surface. *K. brevis* cell numbers were determined microscopically. Aliquots were filtered, under low vacuum (<10 cm Hg), through GF/F (Whatman) glass fiber filters and were quick frozen in liquid nitrogen. Samples were stored at -80°C until later analysis. Filters were analyzed for photosynthetic and photoprotective pigments using high-performance liquid chromatography (HPLC) according to procedures of Wright et al. [1991].

2.2. Inversion of in Situ Absorption Data

Binned absorption data collected by the ac-9 was inverted using the optical signature inversion (OSI) model [Schofield et al., 2004], which estimates the optical concentration of phytoplankton, colored dissolved organic matter (CDOM), and nonalgal particles. The nonalgal particles are dominated by detritus. This is based on inverting the bulk ac-9 absorption using a series of curves that represent the major absorbing components in the water column (Table 1).

Phytoplankton were represented by the mean signatures of high-light and low-light adapted phytoplankton from the three major phytoplankton taxa. The three signatures were for chlorophyll a-c, chlorophyll a-b and phycobilin containing phytoplankton [Johnsen et al., 1994]. While we might have customized the OSI to use *K. brevis* absorption exclusively we decided to use the more general OSI procedure using different phytoplankton taxa as diatoms and unidentified flagellates were present in the low-chlorophyll waters. It should be noted that these species were usually found in water where *K. brevis* numbers were low or not present at all. The CDOM and nonalgal particles were treated as a series of exponential curves [Kalle, 1966; Bricaud et al., 1981; Green and Blough, 1994] where both the optical weight and slopes were allowed to vary. The modeled total absorption represented the sum of the nonalgal, CDOM, and phytoplankton absorption (Table 1). By varying the concentration weights as well as the CDOM and nonalgal particle slopes the difference between modeled and ac-9 measured total absorption spectrum was minimized as a function of wavelength. For this effort, we used an inversion method that included several constraints (Table 1). The constraints ensured that phytoplankton dominated the absorption in the red wavelengths and that the least dominant phytoplankton taxa present was not provided equal weight as the more dominant phytoplankton taxa present [Schofield et al., 2004]. The low presence of the green algae was confirmed with pigment and microscopic analysis. While some of these constraints are admittedly artificial they have been shown to increase the ability of the inversion method to more accurately describe the phytoplankton communities and improve estimates of CDOM and nonalgal particles. The errors of this method have been examined thoroughly [Schofield et al., 2004]. In this study the inverted phytoplankton absorption was calibrated against independent measurements of CDOM in surface waters and chlorophyll fluorescence in the water column. When the OSI method did not

converge on a solution, the data were omitted from the later analysis (<7% of this data set). The stability of the OSI results was also tested by introducing random noise into the ac-9 spectra ($\pm 0.005 \text{ m}^{-1}$ across all wavelengths) and there was no spectral bias and a quantitative impact was less than 2%.

Results

3.1. Field Setting

--- INSERT FIGURE 2 ---

--- INSERT FIGURE 3 ---

--- INSERT FIGURE 4 ---

During the diel study the ship followed the Lagrangian drifter deployed within a patch of *K. brevis*. The water column was shallow (<13 m) and therefore we assume the surface current drifter provided a reasonable trace of the water mass. The salinity and temperature showed only minor salinity changes of 0.25 and less than one degree Celsius, respectively (Figure 2), during the 24 hour diel survey for the entire water column. Given it was a warm day (>25°C) the observed changes in temperature and salinity are roughly consistent with radiant heating and cooling. These changes were significantly less than observed variations between the diel stations and offshore locations several kilometers away (Figure 2). In these different water masses, *K. brevis* cell numbers were much lower. Unfortunately the short duration of this cruise did not allow for extensive mesoscale mapping. Conditions were calm with no perceptible wind and it was generally cloud free during the daylight hours. With low winds there was no perceptible

sediment resuspension. Unfortunately, a persistent marine haze resulted in no useful satellite imagery. Over the diel study, 25 stations were occupied during which bulk absorption increased by almost tenfold in the surface waters with maximum values encountered at 1600 local daylight time (LDT) (Figure 3a). The enhanced bulk absorption peaked in the upper 3 m of the water column. Coincident with the increase in bulk absorption was a threefold increase in *K. brevis* cells (Figure 3b). Chlorophyll a showed a similar diel pattern as the *K. brevis* cell counts and bulk absorption with a threefold increase in surface waters and peak values observed at 1600 LDT (Figure 4a). During this period CDOM increased by ~22% over the 24 hours in the surface waters (note estimates of CDOM increase were similar using estimates from both the LWCC and the ac-9). Also while the cell number and absorption decreased in the early evening, the CDOM values remained high throughout the study (Figure 3b). This increase was largely limited to the surface waters where *K. brevis* dominated the community indicating that the red tide was the likely source of CDOM. The majority of the chlorophyll a increase was associated with *K. brevis* cells as evidenced by significant linear correlations ($p < 0.05$, $R^2 = 0.95$) with the chemotaxonomic carotenoid pigment gyroxanthin diester (Figure 4b) throughout the water column. This chemotaxonomic pigment was linearly correlated with *K. brevis* cell counts (Figure 4c) and the increased bulk absorption in the surface waters during the day.

--- INSERT FIGURE 5 ---

--- INSERT FIGURE 6 ---

--- INSERT FIGURE 7 ---

The inverted optical products (phytoplankton, CDOM and nonalgal particles) showed similar patterns as the bulk properties (Figure 5) and the derived optical weights are proportional

to the concentration of the optically active constituents [Schofield et al., 2004]. Phytoplankton optical weights showed the vertical migration associated with *K. brevis* (Figure 5a). There were significant correlations ($p < 0.05$) between the phytoplankton optical weight and gyroxanthin diester (Figure 6a). Consistent with the surface CDOM measured with LWCC, the inverted ac-9 optical estimates of CDOM showed concentrations increasing during the 24 hours and the increase was not clearly associated the diel migration of *K. brevis* (Figure 5d). There was a significant correlation ($p < 0.05$, $R^2 = 0.53$) between the CDOM absorption estimated by the ac-9 inversion and CDOM absorption measured with the LWCC (Figure 6b). The derived phytoplankton optical weights were significantly correlated with chlorophyll a fluorescence (Figure 7a, $p < 0.05$, $R^2 = 0.93$). The only region where phytoplankton optical weight and fluorescence diverged was in the nearshore surface waters during the daylight hours (Figure 5c). Nonalgal particle optical concentrations showed an inverse relationship with lowest values associated with high phytoplankton concentrations (Figures 5b and 7b). The relationship between phytoplankton and nonalgal particles, and the lack of any relationship between nonalgal particles and CDOM suggests that the inversion model could treat the CDOM and nonalgal particles as independent variables. Only one of the CDOM slope values was unreasonably high (0.04) with the rest of the derived CDOM slopes ranging from 0.012 to 0.025 which reasonably spans published slope values for marine systems [Carder et al., 1989; Roesler et al., 1989].

While the CDOM spectral slope showed no relationship with phytoplankton abundance, the detrital exponential slope showed an inverse relationship with *K. brevis* abundance (Figures 7c and 7d). The optical inversion method constrains the nonalgal particle slope by assuming an upper limit of 0.01 and a lower limit of 0.005. This is admittedly artificial; regardless the low slope values indicate that the lowest nonalgal slopes are associated with the highest

phytoplankton optical weights (Figure 7c). Despite nonalgal particle slopes being low with high concentrations of *K. brevis*, the concentration of nonalgal particles associated with *K. brevis* was also low. The decline of nonalgal particles slopes to a lower limit of 0.005 reflects the lower nonalgal particle limit within the OSI [Schofield et al., 2004].

3.2. Reflectance Associated With *K. Brevis* Blooms

--- INSERT FIGURE 8 ---

--- INSERT FIGURE 9 ---

The hyperspectral reflectance was impacted by the vertical migration of *K. brevis* (Figure 8). The absolute magnitude of the reflectance increased reflecting increased particle backscatter in the surface waters when the *K. brevis* reached the surface (Figure 8a). The relative spectral changes in reflectance were greatest in the green, red and infrared wavelengths of light (Figure 8b). Relative to 400 nm the green light reflectance decreased by 22% during diel migration of *K. brevis* (Figure 8c). In contrast the relative amount of red and infrared wavelengths increased by 75% and 35%, respectively. Reflectance is regulated by the in situ backscattering and absorption properties (to first order $R \sim b_b(\lambda)/[b_b(\lambda) + a(\lambda)]$). The relative amount of backscattering to absorption in *K. brevis* is lower than waters containing little or no *K. brevis* (Figure 9). This decreased backscatter efficiency was evident in the surface waters as *K. brevis* reached the surface during its diel migration (inset in Figure 9). This low backscatter efficiency of *K. brevis* limits the potential increase in reflectance especially at the wavelengths of maximal pigment absorption (Figure 8). Thus the largest changes in reflectance should be in the blue and green wavelengths of lights; however, the decreased absorption of nonalgal particles (an exponential

absorption spectrum decreasing with increasing wavelength) associated with *K. brevis* (Figure 7b) minimizes the relative decrease in the blue wavelengths of light (Figure 8b).

Discussion

Identifying and tracking harmful algal blooms (HABs) is a high priority given the detrimental impacts on coastal communities [Hallegraeff, 1993; Anderson et al., 1998, Kirkpatrick et al., 2004]. Given this, efforts have largely focused on developing remote-sensing techniques that delineate the presence of HABs over ecologically and economically relevant spatial scales [Carder and Steward, 1985; Cullen, 1985; Tester and Steidinger, 1997; Stumpf, 2000; Cannizzaro, 2004; Tomlinson et al., 2004]. These efforts usually define HAB-specific optical properties or identify features that warrant further examination by ship [Schofield et al., 2006]. Many HAB species exhibit significant vertical migration, which allows them to thrive in oligotrophic environments by accessing nutrients at depth [Cullen and Horrigan, 1981] and/or avoiding photoinhibition in the near-surface waters [Walsby et al., 1997]. Many of the other major bloom forming algae in the coastal ocean do not exhibit vertical migration over diurnal timescales. This behavior offers a potentially alternative means to detect HABs; however, the limited revisit intervals of available satellites have not allowed this behavior to be identified using satellites in the past. The constellation of international ocean color satellites is expanding the available satellite imagery and now allows for the possibility of having multiple passes within a single day [Schofield et al., 2002; Glenn and Schofield, 2003]. This capability will improve in the coming years if the geostationary satellites are launched allowing diurnal processes to be monitored. Thus the diurnal temporal dynamics may be an effective means to detect *K. brevis* blooms.

“Red tide” historically refers to the color associated with surface slicks of HABs; however, unraveling the factors that underlie the spectral properties is a complex reflecting the spectral properties of the water column and the physiology of the human eye (H. Diersen, personal communication, 2005). This paper is focused only on the first part of the problem. In HAB populations, changes in the spectral properties reflect several factors including (1) increased absorption by photosynthetic pigments, (2) enhanced chlorophyll fluorescence, (3) changes in the relative composition of colored material associated with the HAB in the water column, and (4) enhanced scattering associated with an increase in particle concentrations at the air-sea interface especially in the near-infrared wavelengths. The importance of these mechanisms varies with wavelength.

There is enhanced red light and infrared reflectance associated with *K. brevis*. One potential source of the red light is chlorophyll a fluorescence. This surface *K. brevis* population exhibited strong fluorescence quenching (Figure 5c) which is consistent with an active xanthophyll cycle known to be active within *K. brevis* [Evens et al., 2001]. During sunny days, such as encountered during this study, fluorescence quantum yields drop close to zero. Therefore the potential contribution of chlorophyll a fluorescence contributing to the red water leaving radiance is low. The second factor influencing the potential red light reflectance results from enhanced scattering associated with a concentrated surface layer of cells. The presence of enhanced backscatter in the surface waters effectively increases red light reflectance by minimizing the absorption of the red and infrared wavelengths of light by water. This process, sometimes referred to as the “Roesler effect,” is best visualized at longer infrared wavelengths where pigment absorption is negligible. During this study, the presence of *K. brevis* in the

surface resulted in a threefold increase in the relative reflectance at 750 nm consistent with the Roesler effect.

Changes in reflectance in the blue and green wavelengths of light are dominated by the absorption of light by phytoplankton, water, nonalgal particles, and CDOM. Pigments associated with surface populations of *K. brevis* decreases reflectance in the bluegreen wavelengths of light; however, the impact on blue light reflectance (<425 nm) appears to be offset by lower absorption by nonalgal particles. This implies a decreased concentration of particles as total absorption is to first order regulated by the amount of particles present. The lower concentration of the nonalgal particles has two impacts on the optical properties in the water column. It has been suggested that compared to other phytoplankton blooms, *K. brevis* blooms exhibit lower backscattering compared to other phytoplankton [Cannizzaro, 2004, Cannizzaro et al., 2004]. The low backscattering efficiency associated with *K. brevis* has been related to its large size (20–40 μm) and a low index of refraction (~ 1.05) [Mahoney, 2003]. The low backscatter efficiency may also reflect other constituents in the water column. The backscattering of light in the ocean is dominated by particles less than 1 μm [Morel and Ahn, 1991; Stramski and Kiefer, 1991], and thus the low backscatter efficiency may also reflect a lower concentration of submicron particles [Ulloa et al., 1994; Twardowski et al., 2001; Cannizzaro, 2004]. The lower concentration of nonalgal particles may be due to the toxicity of *K. brevis* cells which may directly inhibit bacterial growth and/or alter the organic material available for heterotrophic consumption. If low nonalgal particles slopes are indicative of “fresh” nonoxidized detritus material, analogous to low CDOM slopes being indicative of fresh reduced CDOM [Mopper et al., 1991; Kouassi and Zika, 1992; Nelson et al., 1998], then some grazing appears to be present with the *K. brevis* population; however, given the low-concentration nonalgal particles we hypothesize that the

overall grazing rates are low. Grazing rates appear to be low in *K. brevis* blooms [Shuman and Lorenzen, 1975] most likely because of brevetoxin produced by *K. brevis* [Turner and Tester, 1997]. The reduced detritus in turn would lead to a further decline in microbial populations consuming the detritus [Cannizzaro, 2004]. This sequence of events underlies the inverse relationship observed between nonalgal particles absorption and *K. brevis* (Figures 5 and 7).

K. brevis, like many dinoflagellates, is relatively slow growing (2–4 times) compared to other bloom forming phytoplankton taxa [Steidinger et al., 1998]. Despite this, *K. brevis* bloom annually in the Gulf of Mexico [Steidinger et al., 1998] and it has been difficult to explain how *K. brevis* outcompetes faster growing phytoplankton. These mechanisms generally focus on either bottom up regulation driven by the availability of a specific nutrient source (accessing organic nutrient and/or migrating to deep nutrient pools [Steidinger et al., 1998; Walsh and Steidinger, 2001]) or top down regulation (reduced grazing [Turner and Tester, 1997; Kubanek et al., 2005]). While these processes are not mutually exclusive, the optical signatures associated with this *K. brevis* bloom are consistent with the top down regulation of *K. brevis* blooms in the Gulf of Mexico where low detritus loads are associated with depressed grazing rates. This in turn may alter the bacterial communities. Together these processes drive the observed optical impact of *K. brevis* on ocean optics.

Acknowledgments

The crew of the R/V Suncoaster is gratefully acknowledged for the support during this study. The help and partnership of Mote red tide team Barbara Berg, Barbarba Kirkpatrick, and Brad Pederson are toasted with good beer. As always, the support of the Rutgers Coastal Ocean

Observation Lab (COOL) was key to success in the field. The generous support of the EPA and ONR EcoHAB programs is acknowledged. Constructive comments provided by Heidi Dierssen and an anonymous reviewer are acknowledged.

References

Anderson, D. M., A. D. Cembella, and G. M. Hallegraeff (1998), *The Physiological Ecology of Harmful Algal Blooms*, 575 pp., Springer, New York.

Austin, R. W., and T. J. Petzold (1981), The determination of the diffuse attenuation coefficient of sea water using the Coastal Zone Color Scanner, in *Oceanography from Space*, edited by J. F. R. Gower, pp. 239–256, Springer, New York.

Asai, S., J. J. Krzanowski, W. H. Anderson, D. F. Martin, J. B. Polson, R. F. Lockey, S. C. Bukantz, and A. Szentivanyi (1982), Effects of the toxin of red tide, *Ptychodiscus brevis*, on canine tracheal smooth muscle: A possible new asthma-triggering mechanism, *J. Allergy Clin. Immunol.*, 69, 418–428.[CrossRef]

Bricaud, A., A. Morel, and L. Prieur (1981), Absorption by dissolved organic matter of the sea (yellow substance) in the UV and visible domains, *Limnol. Oceanogr.*, 26, 45–53.

Cannizzaro, J. P. (2004), *Detection and quantification of *Karenia brevis* blooms on the West Florida Shelf from remotely sensed ocean color imagery*, Ph.D. dissertation, Univ. of S. Fla., Tampa.

Carder, K. L., and R. G. Steward (1985), A remote-sensing reflectance model of a red-tide dinoflagellate off west Florida, *Limnol. Oceanogr.*, 30, 286–298.

Carder, K. L., R. G. Steward, G. R. Harvey, and P. B. Ortner (1989), Marine humic and fulvic acids: Their effects on remote sensing of chlorophyll a, *Limnol. Oceanogr.*, 34, 68–81.

Cullen, J. J. (1985), Diel vertical migration by dinoflagellates: Roles of carbohydrate metabolism and behavioral flexibility, *Contrib. Mar. Sci.*, 27, 135–152.

Cullen, J., and S. Horrigan (1981), Effects of nitrate on the diurnal vertical migration, carbon to nitrogen ratio, and photosynthetic capacity of the dinoflagellate *Gymnodium splendens*, *Mar. Biol.*, 62, 81–89.[CrossRef]

Eppley, R. W., O. Holm-Hansen, and J. D. H. Strickland (1968), Some observations on the vertical migration of dinoflagellates, *J. Phycol.*, 4, 333–340.

Evens, T. J., G. J. Kirkpatrick, D. F. Millie, D. Chapman, and O. Schofield (2001), Xanthophyll-cycling and photophysiological regulation of *Gymnodinium breve* in response to fluctuating natural irradiance, *J. Plankton Res.*, 23, 1177–1194.

Forward, R. B. (1970), Change in the photoresponse action spectrum of the dinoflagellate *Gyrodinium dorsum* Kofoid by red and far-red light, *Planta*, 92, 245–258.[CrossRef]

Forward, R. B., and D. Davenport (1970), The circadian rhythm of a behavioral photoresponse in the dinoflagellate *Gyrodinium dorsum*, *Planta*, 92, 259–266.[CrossRef]

- Glenn, S. M., and O. Schofield (2003), Observing the oceans from the COOLroom: Our history, experience, and opinions, *Oceanography*, 16, 37–52.
- Green, S. A., and N. V. Blough (1994), Optical absorption and fluorescence properties of chromophoric dissolved organic matter in natural waters, *Limnol. Oceanogr.*, 39, 1903–1916.
- Hallegraeff, G. M. (1993), A review of harmful algal blooms and their apparent global increase, *Phycology*, 32, 79–99.
- Heil, C. A. (1986), Vertical migration of *Ptycodiscus brevis* (Davis) Steidinger, M.S. thesis, 118 pp., Univ. of S. Florida, Tampa.
- Hemmert, W. H. (1975), The public health implications of *Gymnodinium breve* red tides: A review of the literature and recent events, in *Proceedings of the First International Conference on Toxic Dinoflagellate Blooms*, Rep. MITSG 75-8, edited by V. R. LoCicero, pp. 489–497, Mass. Sci. and Technol. Found., Wakefield, Mass.
- Holmes, R. W., P. M. Williams, and R. W. Eppley (1967), Red water in La Jolla Bay, 1964–1966, *Limnol. Oceanogr.*, 12, 503–512.
- Johnsen, G., O. Samset, L. Granskog, and E. Sakshaug (1994), In vivo absorption characteristics in 10 classes of bloom-forming phytoplankton: Taxonomic characteristics and responses to photoadaptation by means to discriminant and HPLC analysis, *Mar. Ecol. Prog. Ser.*, 105, 149–157.
- Kalle, K. (1966), The problem of the gelbstoff in the sea, *Oceanogr. Mar. Biol. Rev.*, 4, 91–104.
- Kamykowski, D. (1981), Laboratory experiments on the diurnal vertical migration of marine dinoflagellates through temperature gradients, *Mar. Biol.*, 62, 57–64.[CrossRef]
- Kamykowski, D. (1995), Trajectories of autotrophic marine dinoflagellates, *J. Phycol.*, 31, 200–208.[CrossRef]
- Kamykowski, D., and H. Yamazaki (1997), A study of metabolism influenced orientation in the diel vertical migration of marine dinoflagellates, *Limnol. Oceanogr.*, 42, 1189–1202.
- Kerfoot, J., G. Kirkpatrick, S. Lohrenz, K. Mahoney, M. A. Moline, and O. Schofield (2005), Vertical migration of a *Karenia brevis* bloom: Implications for remote sensing of harmful algal blooms, in *Harmful Algae: Proceedings of the Xth International Conference on Harmful Algae*, edited by K. A. Steidinger et al., pp. 279–283, Fla. Fish and Wildlife Conserv. Comm., Tampa.
- Kirkpatrick, B., et al. (2004), Literature review of Florida red tide: Implications for human health, *Harmful Algae*, 3, 99–115.[CrossRef]
- Kirkpatrick, G. J., D. F. Millie, M. A. Moline, and O. Schofield (2000), Optical discrimination of a phytoplankton species in natural mixed populations, *Limnol. Oceanogr.*, 45, 467–471.

Kirkpatrick, G. J., C. Orrico, M. A. Moline, M. Oliver, and O. Schofield (2003), Continuous hyperspectral absorption measurements of colored dissolved organic material in aquatic systems, *Appl. Opt.*, 42, 6564–6568.

Kouassi, A. M., and R. G. Zika (1992), Light-induced destruction of the absorbance property of dissolved organic matter in seawater, *Toxicol. Environ. Chem.*, 35, 195–211.

Kubanek, J., M. K. Hicks, J. Naar, and T. A. Villareal (2005), Does the red tide *Karenia brevis* use allelopathy to outcompete other phytoplankton?, *Limnol. Oceanogr.*, 50, 883–895.

Landsberg, J. H., and K. A. Steidinger (1998), A historical review of *Gymnodium breve* red tides implicated in mass mortalities of the manatee (*Trichechus manatus latirostris*) in Florida, USA, in *Proceedings of the 8th International Conference on Harmful Algal Blooms*, edited by B. Reguera et al., pp. 97–100, Vigo, Spain.

Lohrenz, S. E., G. L. Fahnenstiel, G. J. Kirkpatrick, C. L. Carroll, and K. A. Kelly (1999), Microphotometric assessment of spectral absorption and its potential application for characterization of harmful algal species, *J. Phycol.*, 35, 1438–1446.[CrossRef]

Mahoney, K. L. (2003), Backscattering of light by *Karenia brevis* and implications for optical detection and monitoring, Ph.D. dissertation, Univ. of South. Miss., Stennis Space Cent.

Millie, D. F., G. J. Kirkpatrick, and B. T. Vinyard (1995), Relating photosynthetic pigments and in vivo optical density spectra to irradiance for the Florida red-tide dinoflagellate *Gymnodinium breve*, *Mar. Ecol. Prog. Ser.*, 120, 65–75.

Millie, D. F., O. Schofield, G. J. Kirkpatrick, G. Johnsen, P. A. Tester, and B. T. Vinyard (1997), Detection of harmful algal blooms using photopigments and absorption signatures: A case study of the Florida red tide dinoflagellate, *Gymnodinium breve*, *Limnol. Oceanogr.*, 42, 1240–1251.

Mopper, K., X. L. Zhou, R. J. Kieber, R. J. Sikorski, and R. D. Jones (1991), Photochemical degradation of dissolved organic carbon and its impact on the oceanic carbon cycle, *Nature*, 353, 60–62.[CrossRef]

Morel, A. (1988), Optical modeling of the upper ocean in relation to its biogenous matter content (case I waters), *J. Geophys. Res.*, 93, 10,749–10,768.[AGU]

Morel, A., and Y.-H. Ahn (1991), Optics of heterotrophic nanoflagellates and ciliates: A tentative assessment of their scattering role in oceanic waters compared to those of bacteria and algal cells, *J. Mar. Res.*, 49, 177–202.

Nelson, N. B., D. A. Siegel, and A. F. Michaels (1998), Seasonal dynamics of colored dissolved organic material in the Sargasso Sea, *Deep Sea Res., Part I*, 45, 931–957.[CrossRef]

Pegau, W. S., D. Gray, and J. R. V. Zaneveld (1997), Absorption of visible and near-infrared light: The dependence on temperature and salinity, *Appl. Opt.*, 36, 6035–6046.

Pierce, R. H., M. S. Henry, L. S. Proffitt, and P. A. Hasbrouk (1990), Red tide toxin (brevetoxin) enrichment in marine aerosol, in *Toxic Marine Phytoplankton*, edited by E. Graneli et al., pp. 397–402, Elsevier, New York.

Riley, C. M., S. A. Holt, G. J. Holt, E. J. Buskey, and C. R. Arnold (1989), Mortality of larval red drum (*Sciaenops ocellatus*) associated with a *Ptychodiscus brevis* red tide, *Contrib. Mar. Sci.*, 31, 137–146.

Roesler, C. S., M. J. Perry, and K. L. Carder (1989), Modeling in situ phytoplankton absorption from total absorption spectra in productive inland marine waters, *Limnol. Oceanogr.*, 34, 1510–1523.

Roesler, C. S., S. M. Etheridge, and G. C. Pitcher (2006), Application of an ocean color species detection model to the complex red tide communities of the southern Benguela upwelling system, in *Harmful Algae 2002: Proceedings of the Xth International Conference on Harmful Algae*, edited by K. A. Steidinger et al., Fla. Fish and Wildlife Conserv. Comm., Tampa, in press.

Schofield, O., J. Grzymiski, W. P. Bissett, G. J. Kirkpatrick, D. F. Millie, M. A. Moline, and C. S. Roesler (1999), Optical monitoring and forecasting systems for harmful algal blooms: Possibility or pipe dream?, *J. Phycol.*, 35, 1477–1496.[CrossRef]

Schofield, O., T. Bergmann, W. P. Bissett, F. Grassle, D. Haidvogel, J. Kohut, M. A. Moline, and S. Glenn (2002), Linking regional coastal observatories to provide the foundation for a national ocean observation network, *J. Oceanic Eng.*, 27, 146–154.

Schofield, O., T. Bergmann, M. J. Oliver, A. Irwin, G. Kirkpatrick, W. P. Bissett, M. A. Moline, and C. Orrico (2004), Inversion of spectral absorption in the optically complex coastal waters of the Mid-Atlantic Bight, *J. Geophys. Res.*, 109, C12S04, doi:10.1029/2003JC002071.[AGU]

Schofield, O., J. Bosch, S. Glenn, G. Kirkpatrick, J. Kerfoot, S. Lohrenz, M. A. Moline, M. Oliver, and W. P. Bissett (2006), Bio-optics in integrated ocean observing networks: The potential for studying harmful algal blooms, in *Real-Time Observation Systems for Ecosystem Dynamics and Harmful Algal Blooms*, edited by M. Babin, C. S. Roesler, and J. J. Cullen, UNESCO, Paris, in press.

Shuman, F. R., and C. J. Lorenzen (1975), Quantitative degradation of chlorophyll by a marine herbivore, *Limnol. Oceanogr.*, 20, 580–586.

Shumway, S. E., J. Barter, and S. Sherman-Caswell (1990), Auditing the impact of toxic algal blooms on oysters, *Environ. Auditor*, 2, 41–56.

Steidinger, K. A. (1975), Basic factors influencing red tides, in *Proceedings of the First International Conference on Toxic Dinoflagellate Blooms*, Rep. MITSG 75-8, edited by V. R. LoCicero, pp. 153–162, Mass. Sci. and Technol. Found., Wakefield, Mass.

Steidinger, K. A., M. A. Burklew, and R. M. Ingle (1973), The effects of *Gymnodinium breve* toxin on estuarine animals, in *Marine Pharmacology: Action of Marine Biotoxins at the Cellular Level*, edited by D. F. Martine and G. M. Padilla, pp. 179–202, Elsevier, New York.

Steidinger, K. A., G. A. Vargo, P. A. Tester, and C. R. Tomas (1998), Bloom dynamics and physiology of *Gymnodinium breve*, with emphasis on the Gulf of Mexico, in *Physiological Ecology of Harmful Algal Blooms*, edited by E. M. Anderson, A. D. Cembella, and G. M. Hallegraff, pp. 135–153, Springer, New York.

Stramski, D., and D. A. Kiefer (1991), Light scattering in microorganisms in the open ocean, *Prog. Oceanogr.*, 28, 343–383.[CrossRef]

Stumpf, R. P. (2000), Applications of satellite ocean color sensors for monitoring and predicting harmful algal blooms, *J. Hum. Ecol. Risk Assess.*, 7, 1363–1368.[CrossRef]

Tester, P. A., and K. A. Steidinger (1997), *Gymnodinium breve* red tide blooms: Initiation, transport, and consequences of surface circulation, *Limnol. Oceanogr.*, 42, 1039–1051.

Tomlinson, M. C., R. P. Stumpf, V. Ransibrahmanakul, E. W. Turby, G. J. Kirkpatrick, B. A. Pederson, G. A. Vargo, and C. A. Heil (2004), Evaluation of the use of SeaWiFS imagery for detecting *Karenia brevis* harmful blooms in the eastern Gulf of Mexico, *Remote Sens. Environ.*, 91, 293–303.[CrossRef]

Turner, J. T., and P. A. Tester (1997), Toxic marine phytoplankton, zooplankton grazers, and pelagic food webs, *Limnol. Oceanogr.*, 42, 1203–1214.

Twardowski, M. S., E. Boss, J. B. Macdonald, W. S. Pegau, A. H. Barnard, and J. R. V. Zaneveld (2001), A model for estimating bulk refractive index from the optical backscattering ratio and the implications for understanding particle composition in case I and case II waters, *J. Geophys. Res.*, 106, 14,129–14,142.[AGU]

Tyler, M. A., and H. H. Seliger (1981), Selection for a red tide organism: Physiological responses to the physical environment, *Limnol. Oceanogr.*, 26, 310–332.

Ulloa, O., S. Sathyendranath, and T. Platt (1994), Effect of the particle-size distribution on the backscattering ratio in seawater, *Appl. Opt.*, 33, 7070–7077.

Walsby, A. E., P. K. Hayes, R. Boje, and L. Stahl (1997), The selective advantage of buoyancy provided by gas vesicles for planktonic cyanobacteria in the Baltic Sea, *New Phytol.*, 136, 407–417.[CrossRef]

Walsh, J. J., and K. A. Steidinger (2001), Saharan dust and Florida red tides: The cyanophyte connection, *J. Geophys. Res.*, 106, 11,597–11,612.[AGU]

Wright, S. W., S. W. Jeffrey, R. F. C. Mantoura, C. A. Llewellyn, T. Bjornland, D. Repeta, and N. Welschmeyer (1991), Improved HPLC method for the analysis of chlorophylls and carotenoids from marine phytoplankton, *Mar. Ecol. Prog. Ser.*, 77, 183–196.

Figures

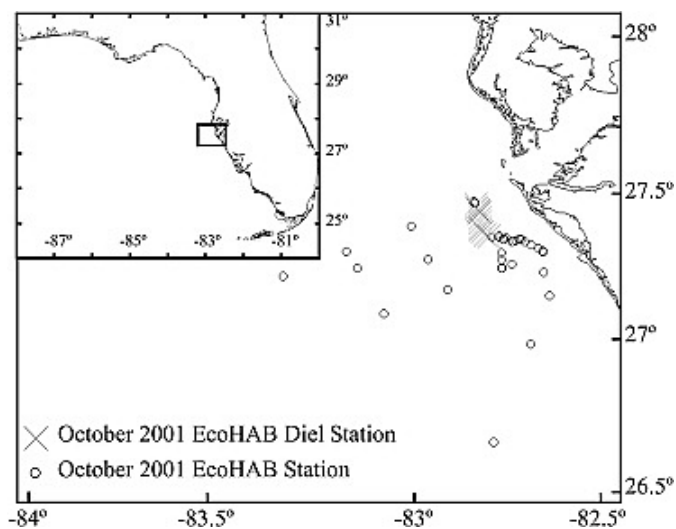


Figure 1. Location of the Ecology of Harmful Algal Blooms (EcoHAB) study conducted in October 2001. The study consisted of a mesoscale survey with occasional survey stations (denoted by open circles) and a 24 hour diel study (gray crosses). Enhanced TIF [399 KB]

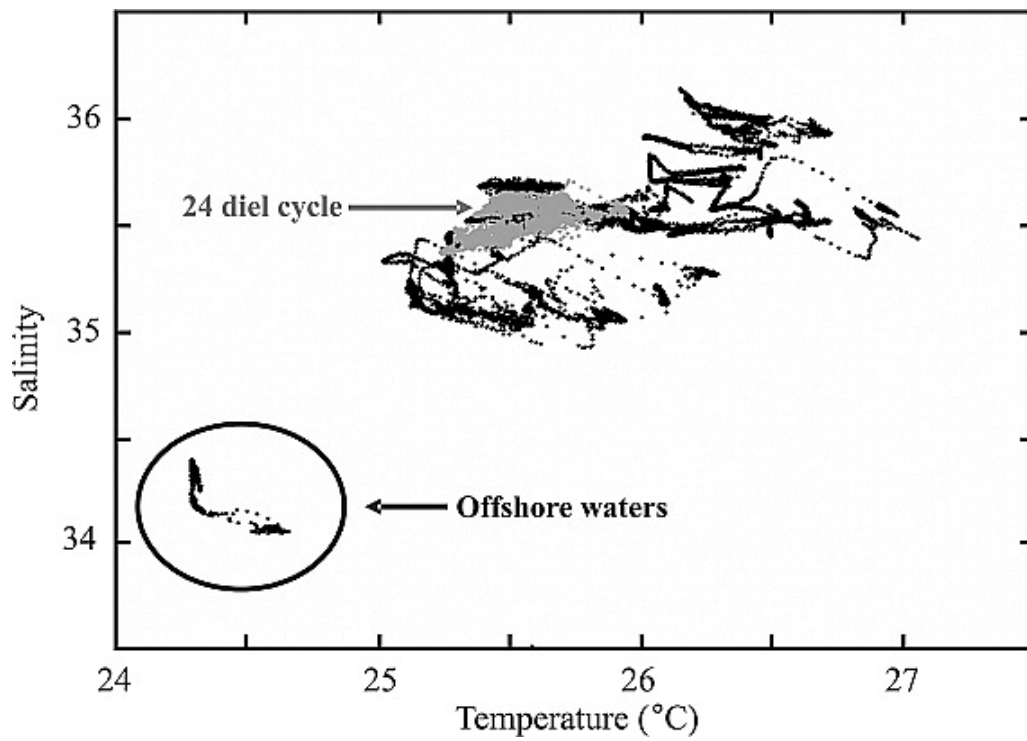


Figure 2. Temperature salinity plot for the discrete stations during this cruise. The gray symbols indicate the temperature and salinities encountered during the diel study. Enhanced TIF [1.0 MB]

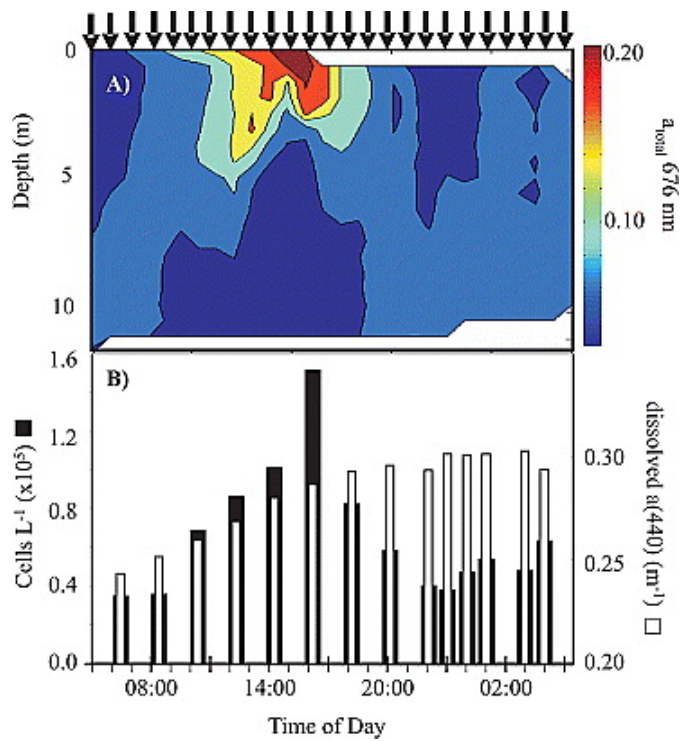


Figure 3. (a) Bulk absorption at 676 nm measured with the ac-9 during the 24 diel cycle. The times of the profile and discrete data collection are indicated by the black arrows. The absorption increased in the upper 2 m of the water column with magnitudes peaking at 1600 LDT. (b) Time series of *K. brevis* cell counts (solid bars) and LWCC measured CDOM absorption at 440 nm (open bars) in surface waters during the diel study. Enhanced TIF [320 KB]

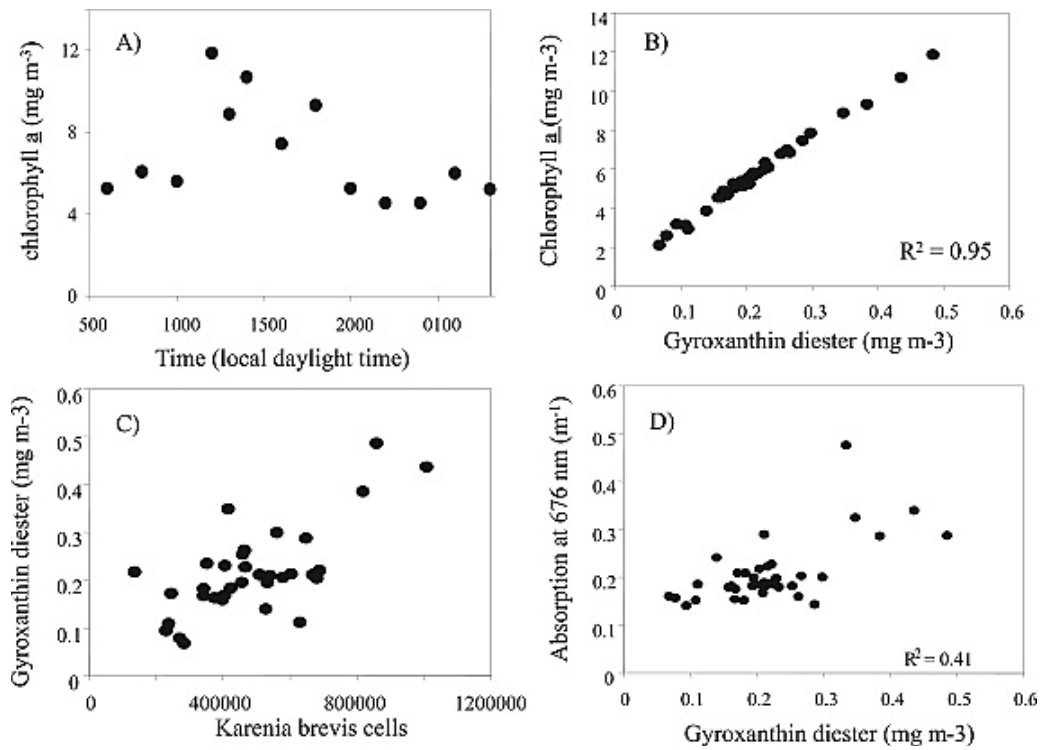


Figure 4. Comparison of discrete biological data collected at all depths. (a) Time series of surface waters chlorophyll a (mg m^{-3}) during the diel study. (b) Significant correlation between chlorophyll a and the *K. brevis*-specific carotenoid gyroxanthin diester. (c) Significant correlation between gyroxanthin diester and *K. brevis* cell counts. (d) Significant correlation between bulk absorption at 676 nm and gyroxanthin diester. Enhanced TIF [2.6 MB]

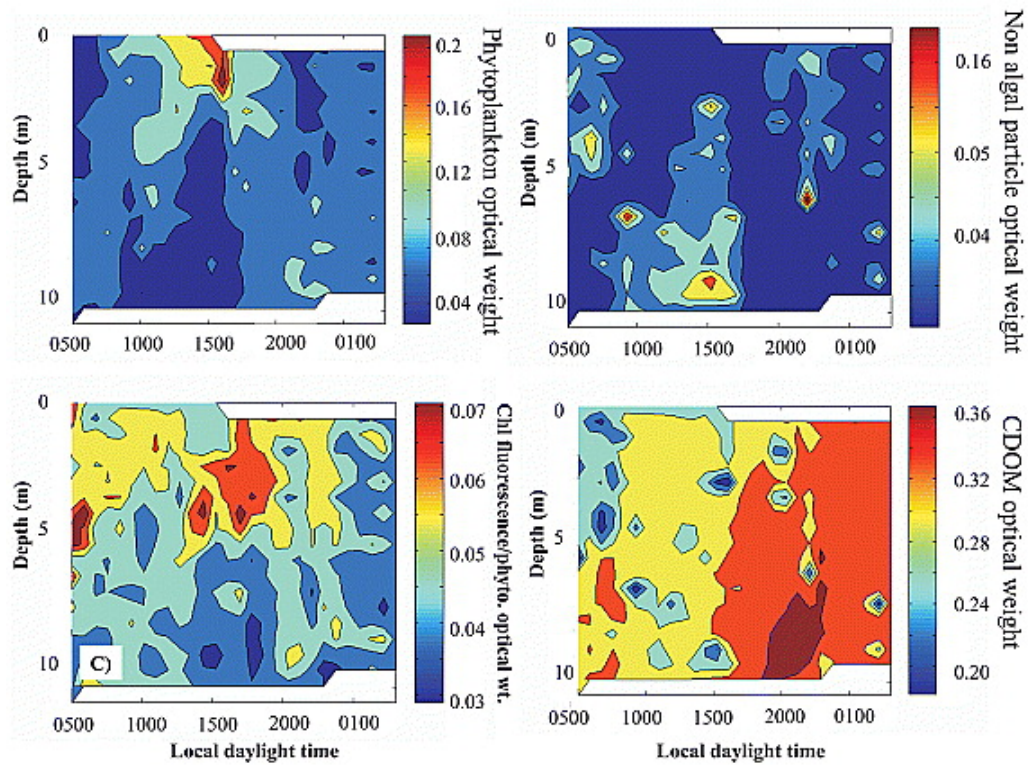


Figure 5. (a) Diel time series for the inverted ac-9 estimate for phytoplankton abundance. (b) Diel time series for the inverted ac-9 estimate of nonalgal particle optical abundance. (c) Diel time series for the ratio of chlorophyll a fluorescence to phytoplankton optical concentration. (d) Diel time series for the inverted ac-9 estimate of CDOM optical abundance. Enhanced TIF [2.8 MB]

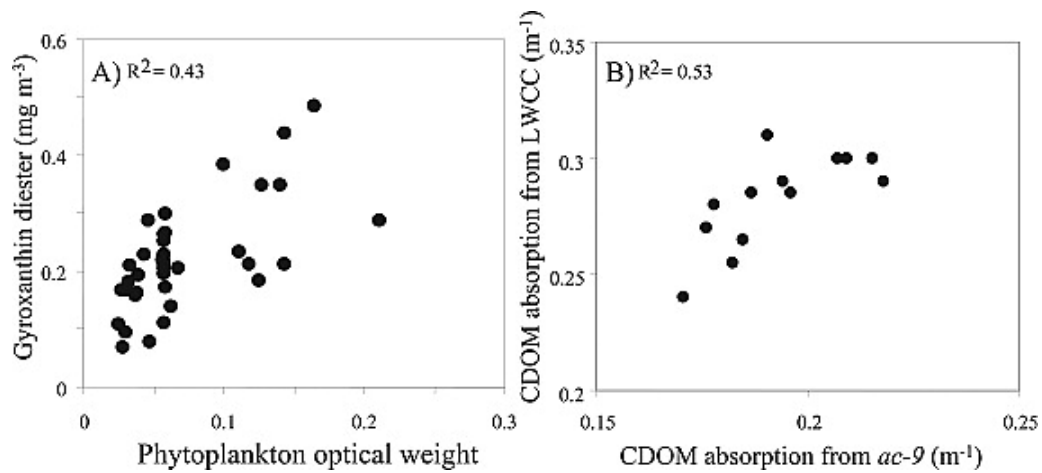


Figure 6. (a) Significant correlation between the gyroxanthin diester (mg m^{-3}) and the phytoplankton optical weight ($p < 0.05$). Not shown but an equally significant regression was observed between the phytoplankton optical weight and chlorophyll a. (b) Significant correlation between CDOM absorption (m^{-1} at 440 nm) estimated with the *ac-9* inversion and CDOM absorption (m^{-1} at 440 nm) measured with ship-based LWCC. Enhanced TIF [287 KB]

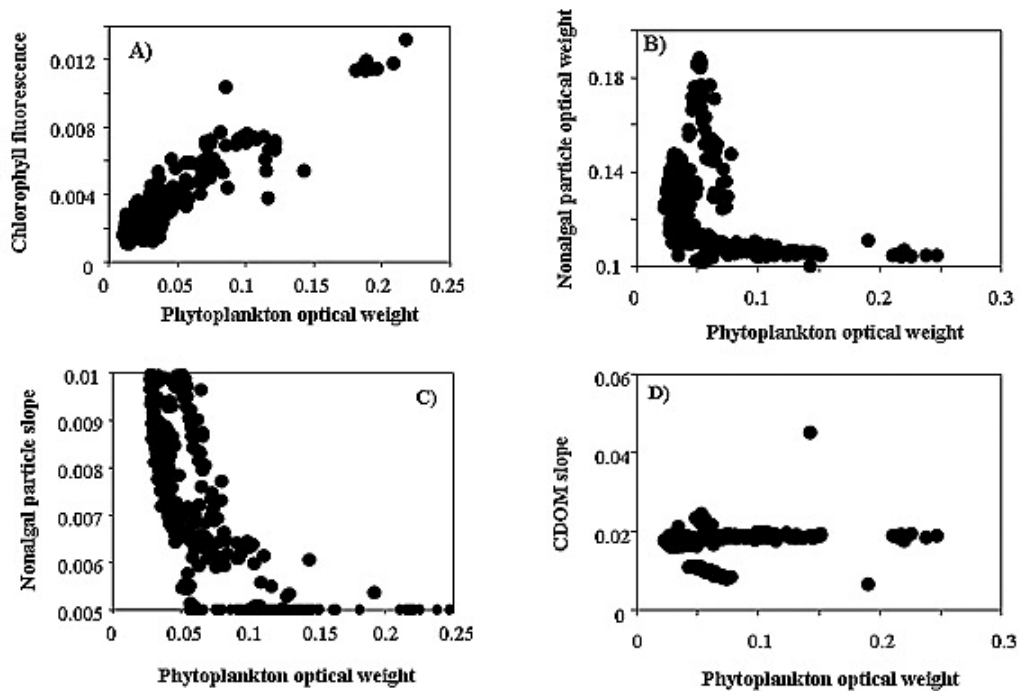


Figure 7. (a) Significant linear correlation between the ac-9 derived phytoplankton optical concentration and chlorophyll a fluorescence. (b) Relationship between phytoplankton and the nonalgal particle optical abundances. (c) Relationship between nonalgal particle exponential slope and phytoplankton abundance. (d) Relationship between the CDOM exponential slope and phytoplankton abundance. Enhanced TIF [512 KB]

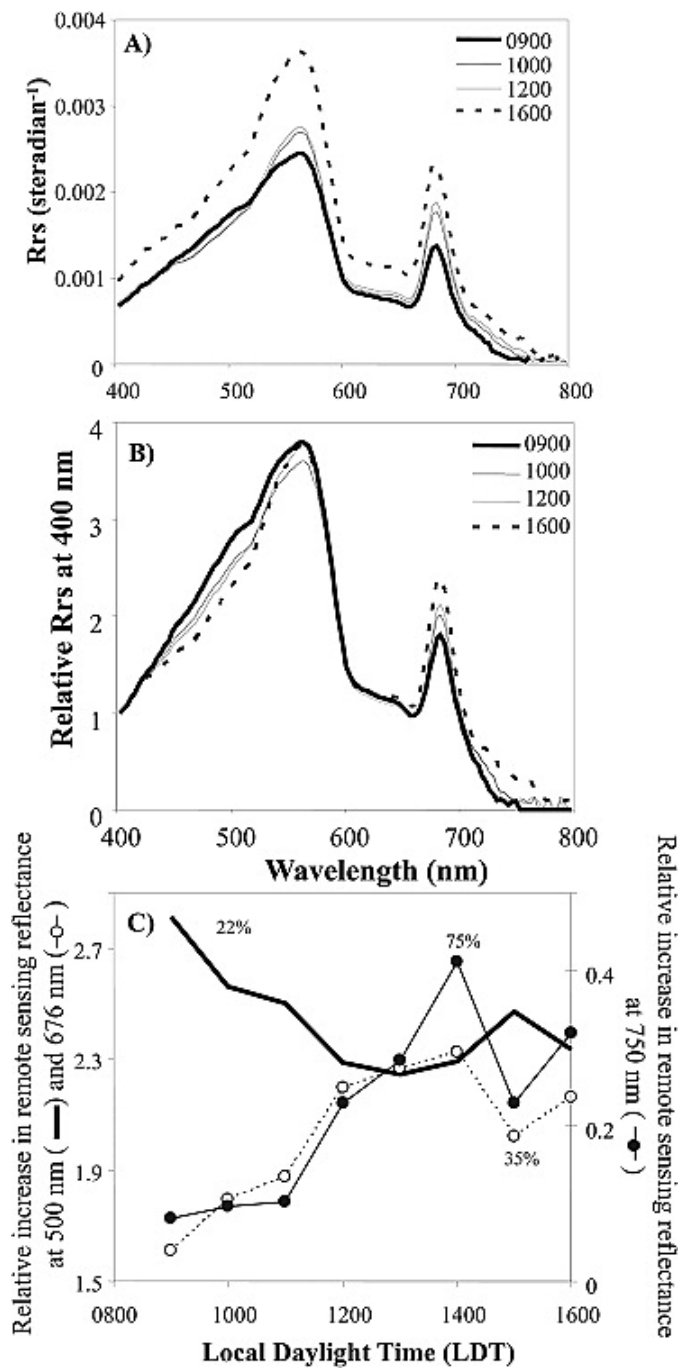


Figure 8. (a) Remote-sensing reflectance during the diel migration of the *K. brevis*. (b) Spectral remote-sensing reflectance normalized to values at 400 nm during the diel migration of *K. brevis*. (c) Relative change in reflectance at 500 nm (bold line), 676 nm (open circles), and 750 nm (closed circles) during the diel study. Enhanced TIF [509 KB]

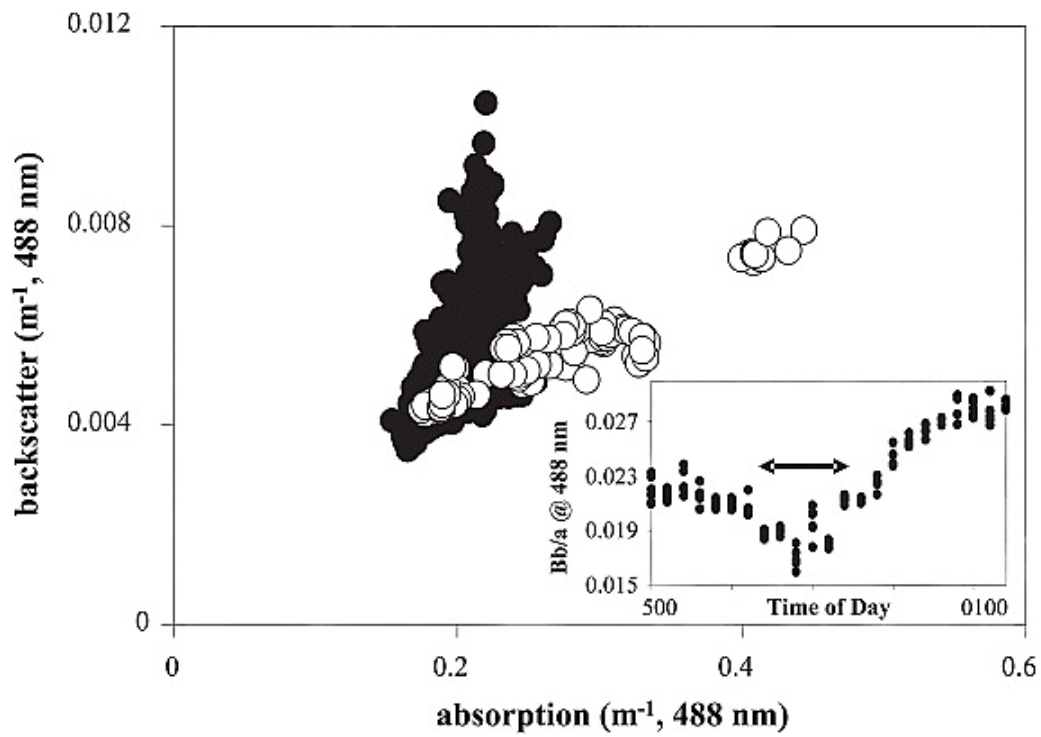


Figure 9. Relationship backscatter and absorption at 488 nm for the entire cruise. The black circles indicate waters with low *K. brevis* cell concentrations, and the open circles indicate waters with high *K. brevis* concentrations. The inset shows the 24 hour time series in the high *K. brevis* waters showing the depression in the backscatter to absorption ratio as cells migrate into the surface waters. Enhanced TIF [485 KB]

Table 1. Constraints and Equations Used by the ac-9 Inversion Method^a

Equations and Constraints Used in the Inversion	
Equations	
Equation (1)	$a(\text{total})_{\text{ac9}} = w_1 \cdot a_{\text{phyto1}}(\lambda) + w_2 \cdot a_{\text{phyto2}}(\lambda) + w_3 \cdot a_{\text{phyto3}}(\lambda) + w_4 \cdot a_{\text{cdom}}(\lambda, s) + w_5 \cdot a_{\text{nonalg alparticles}}(\lambda, r)$
Equation (2)	$a_{\text{CDOM}}(\lambda) = a_{\text{CDOM}} \exp[-s \cdot (\lambda - 412\text{nm})]$
Equation (3)	$a_{\text{nonalg alparticles}}(\lambda) = a_{\text{nonalg alparticles}} \exp[-r \cdot (\lambda - 412\text{nm})]$
Constraints	
Constraint 1	$w_1 \cdot a_{\text{phyto1}}(\lambda), w_2 \cdot a_{\text{phyto2}}(\lambda), w_3 \cdot a_{\text{phyto3}}(\lambda), w_4 \cdot a_{\text{cdom}}(\lambda, s), w_5 \cdot a_{\text{nonalg alparticles}}(\lambda, r) > 0$
Constraint 2	$w_5 \cdot a_{\text{cdom}}(676\text{nm}, s) = w_5 \cdot a_{\text{nonalg alparticles}}(676\text{nm}, r)$
Constraint 3	$s \geq r$
Constraint 4	$w_1 \cdot a_{\text{phyto1}}(\lambda) \geq w_4 \cdot a_{\text{CDOM}}(676\text{nm}, s) + w_5 \cdot a_{\text{nonalg alparticles}}(676\text{nm}, r) \geq 0$
Constraint 5	$w_2 \cdot a_{\text{phyto2}}(\lambda) \geq w_4 \cdot a_{\text{CDOM}}(676\text{nm}, s) + w_5 \cdot a_{\text{nonalg alparticles}}(676\text{nm}, r) \geq 0$
Constraint 6	$w_1 \cdot a_{\text{phyto1}}(\lambda) \geq w_3 \cdot a_{\text{phyto3}}(\lambda)$
Constraint 7	$w_2 \cdot a_{\text{phyto2}}(\lambda) \geq w_3 \cdot a_{\text{phyto3}}(\lambda)$
<p>^aSee Schofield et al. [2004] for a complete description and error analysis of the inverter results. The values of w_1, w_2, w_3, w_4, and w_5 are nonspectrally dependent scalar coefficients of input spectra. We used fixed absorption spectra (w_1 is chlorophyll a minus chlorophyll c algal absorption, w_2 is chlorophyll a minus chlorophyll b algal absorption, and w_3 is phycobilin algal absorption) measured on laboratory cultures in order to ensure that inversion was completely independent from any spectral curves encountered in the field. Estimates of CDOM and non-algal particles optical weights were w_4 and w_5, respectively, and were combined as a series of exponential slopes (s and r). The equations and constraints used by the inverter are listed below. A full description of the reasons and impacts of the constraints are discussed by Schofield et al. [2004].</p>	

